

Journal of Engineering Technology and Applied Physics

Simulations for the Susceptible-Exposed-Infected-Recovered (SEIR) Model in the Forecast of Epidemic Outbreak

Mei Feng Liu* and Boo Hui Ling

Department of Mathematics, School of Mathematics and Physics, Xiamen University Malaysia, Selangor, Malaysia.

*Corresponding author: meifeng@xmu.edu.my, ORCID: 0000-0002-8763-8300

<https://doi.org/10.33093/jetap.2024.6.1.11>

Manuscript Received: 15 August 2023, Accepted: 30 November 2023, Published: 15 March 2024

Abstract—Mathematical modelling based on the compartmental Susceptible – Exposed – Infected - Recovered (SEIR) model is proposed in this paper to study the pandemic outbreak. In addition, simulations from both the deterministic approach as well as the stochastic approach are implemented to validate the present study. Among each state, the transitions between different categories are simulated by using various graph models including the complete graph, the steady Erdos-Renyi graph, as well as the varying Erdos-Renyi graph. The related parameters for the SEIR model are chosen from available literature and the effect of some other factors such as the inflow or outflow of travellers in a city as well as the impact of vaccination rate is explored. Furthermore, the difference between the simulation results coming from the deterministic SEIR model and the stochastic SEIR one is examined to check the availability of the present simulation. It is found that, the stochastic simulation based on the complete graph is more consistent with the deterministic SEIR model.

Keywords—Epidemic Outbreak, SEIR Model, Complete Graph, Steady Erdos-Renyi Graph, Varying Erdos-Renyi Graph

I. INTRODUCTION

A susceptible-infectious-recovered (SIR) model is used in [1] to simulate the infectious trend and trajectory of COVID-19 to understand the severity of the disease as well as to estimate the approximate number of days required for the trend to decline in Malaysia. The transmission rate, β , is used to predict the cumulative number of infectious individuals. The study findings indicate that outbreak control measures such as Movement Control Order (MCO), social distancing implementation and increased hygienic

awareness are essential in controlling the spread of the pandemic outbreak in Malaysia.

The simple but fundamental SIR model has been used to generate important insights about the evolution of a new epidemic in an idealized susceptible population with random connection. However, for most infectious diseases, there is a latent period between being infected and becoming infected, i.e., the exposed category (E). It is reasonable to add the E state into the SIR model in order to account for the complex disease transmission scenarios and the complicated flows between them.

The susceptible-exposed-infectious-recovered (SEIR) model is implemented in [2] to estimate the infected population and the number of casualties of epidemic disease caused by highly contagious coronavirus that has spread in Northern Italy. A case study is performed rigorously in view of the lack of suitable data and the uncertainty of the different parameters. The said analysis shows how isolation measures, social distancing, and knowledge of the diffusion conditions are useful in understanding the dynamics of the epidemic.

A SEIR model is used by [3] to study the worldwide COVID-19 pandemic outbreak in terms of exposed, infected, recovered/deceased, and original confirmed cases as well as to predict the future outbreak of COVID-19 in specific countries such as Hubei Province, China; Taiwan; South Korea; Japan and Italy. In order to calculate the number of confirmed cases in each country, four differential equations are applied, and the results are plotted; in addition, polynomial regression with the logic of

multiple linear regression is also exploited to forecast the further spreading of the pandemic. The calculated and predicted cases of the confirmed population are plotted, and the perfect true results for the future spreading of the pandemic is observed from the intersection of the lines of calculated and predicted cases.

A mathematical SEIR model with a restriction parameter is used in [4] to explore the dynamic of the COVID-19 pandemic. A nonlinear and robust control algorithm based on variable structure control (VSC) for controlling the transmission of COVID-19 is proposed in that study. The VSC algorithm is essential in defining a switching surface and there are three switching surfaces which depend on the different combinations of susceptible, exposed, infected and total population.

An extended SEIR model with a vaccination compartment is proposed in [5] to simulate the spreading of the novel coronavirus disease (COVID-19) in Saudi Arabia, in which seven stages of infection involving susceptible (S), exposed (E), infectious (I), quarantined (Q), recovered (R), deaths (D), and vaccinated (V) are considered. A data assimilation method named ensemble Kalman filter (EnKF) is used to constrain the model outputs and its parameters with available data. Meanwhile, the joint state-parameters estimation experiments with daily data are conducted for enhancing the model's forecasting skills. Numerical results show that the proposed model is capable to achieve accurate prediction of the epidemic development up to two-week time scales, and the number of confirmed cases and deaths are significantly decreased by intensifying the vaccination campaign.

The objective of this paper is to perform the pandemic simulations based on SEIR model in both deterministic and stochastic approaches. In addition, different modes of interaction between each state (category) will be simulated by using Complete Graph, steady Erdos-Renyi graph, and the varying Erdos-Renyi graph theory. Moreover, differences between the deterministic model and the stochastic SEIR model will be analysed and compared. Lastly, related parameters will be investigated, and some other factors including vaccination rate and inflow or outflow rate due to traveling will be explored.

II. SEIR MODEL

As one of the fundamental ideas for the mathematical modelling of epidemiology related to the transmission of infectious diseases, SEIR model is commonly used to simulate the outbreak of a pandemic. In the SEIR model, the population will be classified into four categories, respectively Susceptible (S), Exposed (E), Infected (I), and Recovered (R). A typical schema scenario for these four states/ categories is depicted in Fig. 1.

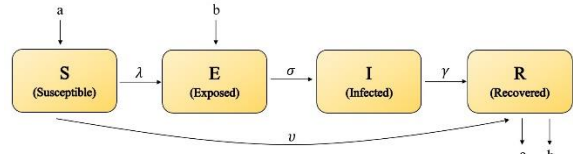


Fig. 1. Disease transmission flow of the proposed SEIR model.

Each category in the SEIR model is described as below:

- Susceptible category S , consists of the total number of individuals who are susceptible to the disease.
- Exposed category E , represents the total number of individuals who are exposed to the disease. They are individuals who are in contact with the infected individuals and become infectious with an incubation rate, σ .
- Infected category I , denotes the total number of individuals who are infected with the disease and are capable of spreading and infecting others with the disease.
- Recovered category R , expresses the total number of individuals who are recovered from the disease and can be removed from the system. Normally, the individuals who are recovered will not flow back to category S since they are assumed to have immunity to the disease.

A. Deterministic SEIR Model

Since the total population, $N = S + E + I + R$ is likely to be large, instead of dealing with such large numbers, we will simplify the computation by dividing each category with N and thus calculating the proportion of each category. A system of ordinary differential equations (ODEs) for the SEIR model in terms of the function $s(t)$, $e(t)$, $i(t)$ and $r(t)$ is given by

$$\begin{aligned}
 s'(t) &= -\beta s(t)i(t), \\
 e'(t) &= \beta s(t)i(t) - \sigma e(t), \\
 i'(t) &= \sigma e(t) - \gamma i(t), \\
 r'(t) &= \gamma i(t),
 \end{aligned} \tag{1}$$

where s denotes the proportion of individuals in category S , e represents the proportion of individuals in category E , i denotes the proportion of individuals in category I , r represents the proportion of individuals in category R and t is the time variable. Related parameters are defined as below:

- λ : Exposure rate (rate at which a suspected person becomes exposed). It is the product of the rate of contact, β and the probability of infection given that contact occurred, in particular, $\lambda = \frac{\beta I}{N}$.
- β : Transmission rate (rate of contact).
- σ : Incubation rate (rate at which an exposed person becomes infected).
- γ : Recovery rate (rate at which an infected person becomes recovered).

B. Equilibria

An equilibrium state happens when the values of the $s'(t), e'(t), i'(t)$ and $r'(t)$ in Eq. (1) are equal to zero, in particular, the system is likely to enter an exact equilibrium with no more changes and is given by

$$\begin{bmatrix} s'(t) \\ e'(t) \\ i'(t) \\ r'(t) \end{bmatrix} = \begin{bmatrix} -\beta s i \\ \beta s i - \sigma e \\ \sigma e - \gamma i \\ \gamma i \end{bmatrix} = \begin{bmatrix} 0 \\ 0 \\ 0 \\ 0 \end{bmatrix}. \quad (2)$$

After solving the system of Eq. (2), it can be easily found that, at equilibrium state, the solutions of our SEIR model are given by

$$s \equiv \text{constant}, e = i = 0, r \equiv \text{constant}.$$

Since $e = i = 0$, all equilibria of our SEIR model are known as disease-free equilibria. When there is an infection and it never disappears from the population, such equilibria are known as endemic equilibria since the disease is endemic.

Suppose that N represents a city's population and assumes that travel into and out of the city is allowed. Then, it is appropriate to consider adding some terms that represent the influx of travellers in some category, that is, the number of people entering minus the number of people leaving. By adding a small influx into susceptible category S , and exposed category E , of our SEIR model, even if we assume that infected people do not travel, there will still be an effect on the disease-free equilibrium of our model. Let a be the influx of travellers in susceptible category S and b be the influx of travellers in exposed category E . By adding a and b to our ODE system, we have

$$\begin{aligned} s'(t) &= -\beta s(t)i(t) + a, \\ e'(t) &= \beta s(t)i(t) - \sigma e(t) + b, \\ i'(t) &= \sigma e(t) - \gamma i(t), \\ r'(t) &= \gamma i(t) - (a + b). \end{aligned} \quad (3)$$

Since the influxes a and b are added into the categories S and E , respectively and suppose that $N = S + E + I + R$, where the total population, N , is constant, the influxes a and b are subtracted from the last equation $r'(t)$ in Eq. (3).

C. Basic Reproductive Number, R_0

A basic reproduction number, denoted as R_0 , is the classical epidemiological measure that used to indicate the reproductive power of the disease, that is, the expected number of infected persons in a population that is completely susceptible. It indicates whether or not the infection will spread throughout the population. R_0 provides a threshold for the stability of the disease-free equilibrium point, that is, when $R_0 > 1$, the disease-free equilibrium is not stable, when $R_0 < 1$, the disease-free equilibrium is stable.

Since R_0 is a threshold that used to determine the stability of the disease-free equilibrium point, it implies that R_0 can be used to determine whether an epidemic outbreak is expected to occur or not. At

equilibrium state, the ODE system for the SEIR model is given by Eq. (2) and can be solved, in which we can find that

$$s \equiv \text{constant}, \quad e = i = 0, \quad r = \text{constant}.$$

Here, we let $s = s_0$ and $r = r_0$, where s_0 and r_0 are constants. By adding up the equations de/dt and di/dt in Eq. (2), we have

$$\frac{d(e+i)}{dt} = (\beta s - \gamma)i. \quad (4)$$

From Eq. (4), if we assume that i is a small positive value, then the value of $e + i$ will decrease to its equilibrium value only when $\beta s_0 - \gamma$ is negative, that is, $\beta s_0 - \gamma < 0$. Then, we have

$$\beta s_0 - \gamma < 0.$$

Rearranging the terms, we find

$$\beta s_0 < \gamma.$$

If we assume that $s_0 = 1$, that is the whole total population, N , we find

$$\beta - \gamma < 0 \Rightarrow \beta < \gamma.$$

By dividing γ on both sides of the inequality, we find

$$\frac{\beta}{\gamma} < 1.$$

Since the basic reproductive of our SEIR model, R_0 is given by

$$R_0 = \frac{\beta}{\gamma} s_0,$$

and assume that $s_0 = 1$, we find $R_0 < 1$.

We show that if $R_0 < 1$, then $e + i$ will decrease and the disease-free equilibrium is stable. Conversely, if $R_0 > 1$, then $e + i$ will increase and the disease-free equilibrium is not stable. In particular, when $R_0 > 1$, an epidemic outbreak could be expected, when $R_0 < 1$, there is no epidemic outbreak.

Although our model does not consider the impact of vaccination, we will still have a small discussion about it. Let ν represents the vaccination rate and assume that ν of the population are vaccinated, then that population will move directly from category S to category R . In other words, the initial individual in category S , s_0 will become $s_0(1 - \nu)$. Also, the basic reproductive number, R_0 is revised to $R_0 = \beta s_0(1 - \nu)$. So, if we have a sufficiently large population who have been vaccinated, then it is said to be effective to prevent an epidemic outbreak since when ν is sufficiently large, the value of R_0 will be less than 1, that is, no epidemic outbreak.

III. SIMULATIONS AND RESULTS

In this section, numerical solutions for the deterministic SEIR model and simulations for the stochastic SEIR compartmental will be presented. All

the simulation results of the stochastic SEIR model will be compared with the numerical solutions of the SEIR equations in order to see if the simulation is expedient.

A. Deterministic SEIR Model

The numerical solutions to the system of ordinary different equations for the SEIR model, say Eq. (1), are solved by using Explicit Runge-Kutta method of order 5(4), and implemented in Python via importing the `solve_ivp` package, a package belongs to `scipy.integrate`. The approximate results for the curves of each category versus time are presented in Fig. 2, in which the adopted parameters are as follows [6]:

- Transmission rate: $\beta = 2.2 \gamma$,
- Incubation rate: $\gamma = 1/5.2$,
- Recovery rate: $\gamma = 1/2.3$,
- Initial population in category *S*: $s(0) = 0.99$,
- Initial population in category *E*: $e(0) = 3(0.02)/100$,
- Initial population in category *I*: $i(0) = 0.02/100$,
- Initial population in category *R*: $r(0) = 0$,
- Time domain: $t = 100$ days.

It can be seen from Fig. 2 that during the first few time steps, the number of suspected individuals decreases slowly, and the number of exposed individuals increases slowly as well. This is because the transmission is just beginning and not too many infected individuals will be contacted. However, as time goes by and the outbreak starts, it is obvious that a dramatic drop for the suspected category and a sharp rise for the exposed one can be detected. After the middle of the time span, the number of recovered individuals surpasses the number of suspected individuals, which implies that the pandemic is about to diminish. The number of exposed and infected individuals is comparably lower than that of suspected and recovered ones, and both reach a peak roughly in the vicinity of the golden cross.

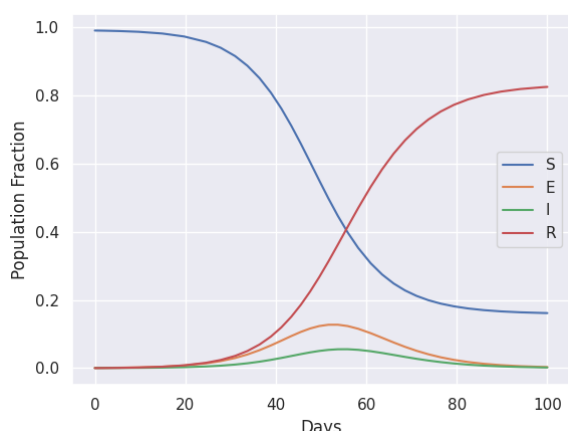


Fig. 2. SEIR model with $\beta = 2.2\gamma$, $\sigma = 1/5.2$, $\gamma = 1/2.3$, $s(0) = 0.99$, $e(0) = 3(0.02)/100$, $i(0) = 0.02/100$, $r(0) = 0$ and $t = 100$ days.

To explore the effect of influxes of travelers on the results of the deterministic SEIR model, the initial value problem introduced in Eq. (3) is further solved by using the `solve_ivp` package with the same setting of parameters as in Fig. 2 with additional influxes $a = 0.005$ and $b = 0.001$. From Fig. 3, it is observed that during the first 10 days, the number of suspected individuals increases, and the value of population fraction exceeds 1.0 as influx a is added to category *S*. Also, the number of recovered individuals during the first 18 days decreases and has a population fraction value that is less than 0 as influxes a and b are subtracted from category *R*. The number of recovered individuals surpasses the number of suspected individuals roughly at $t = 39$ days, which appears earlier than the one without influxes a and b as presented in Fig. 2. The number of exposed and infected individuals is comparably lower than that of suspected and recovered ones, and both reach a peak roughly at $t = 35$ days which is also earlier. In comparison to the model without influxes a and b , the peak number of exposed and infected individuals are doubled. This is because the total number of the population has largely increased due to influxes a and b .

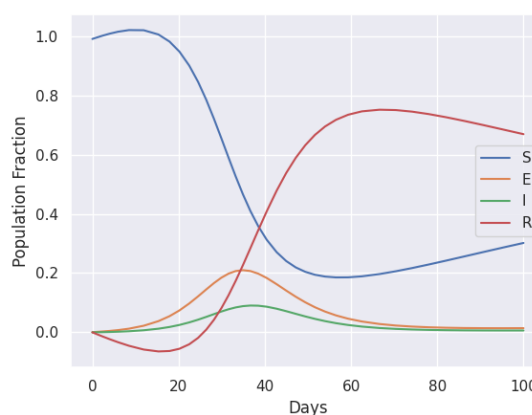


Fig. 3. SEIR model with $\beta = 2.2\gamma$, $\sigma = 1/5.2$, $\gamma = 1/2.3$, $s(0) = 0.99$, $e(0) = 3(0.02)/100$, $i(0) = 0.02/100$, $r(0) = 0$, $t = 100$ days, $a = 0.005$ and $b = 0.001$.

To look into the effect of vaccination rate on the results of the deterministic SEIR model, Eq. (1) is solved by using the `solve_ivp` package with the same setting of parameters as Fig. 2, except s_0 is replaced by $s_0(1 - \nu)$ and ν is 0.50. From Fig. 4, the trend of curves *S*, *E*, *I*, and *R* is similar to the one in the previous case. The main difference between the SEIR models with and without vaccination rates is the reduction in the initial population of category *S*. When $t = 0$, there are $s_0\nu$ individuals in category *S* who are vaccinated and will be directly moved into category *R*, thus there will be $s_0(1 - \nu)$ individuals in category *S*. The number of recovered individuals surpasses the number of suspected individuals roughly at $t = 48$ days, which is slightly earlier than the one without vaccination rate. The peak numbers of exposed

individuals and infected individuals are half of the model without vaccination rate.

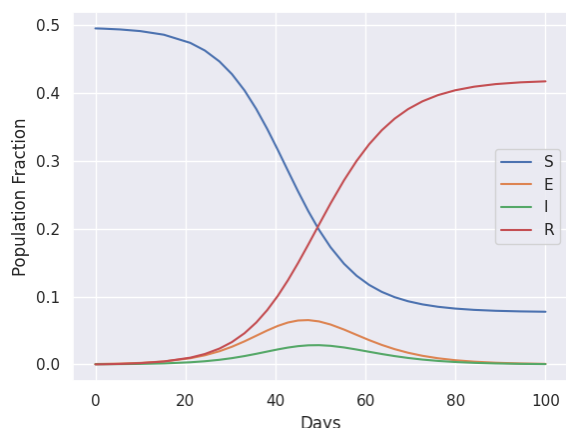


Fig. 4. SEIR model with $\beta = 2.2\gamma$, $\sigma = 1/5.2$, $\gamma = 1/2.3$, $s(0) = 0.99(1 - \nu)$, $e(0) = 3(0.02)/100$, $i(0) = 0.02/100$, $r(0) = 0$, $t = 100$ days and $\nu = 0.50$.

As for the effect of basic reproductive number R_0 on the epidemic outbreak, the behaviour of each category subjected to various values of β is investigated in the following cases, where R_0 is related to β by $R_0 = \frac{\beta}{\gamma}s_0$. Firstly, the case when $R_0 > 1$ is considered. To investigate the effect of the values β on the results of the deterministic SEIR model, Eq. (1) is solved by using the `solve_ivp` package with the same setting of parameters as in Fig. 2, but $\beta = 2.2\gamma$ is revised into $\beta = 2.5\gamma$, $\beta = 2.0\gamma$ and $\beta = 1.5\gamma$ respectively.

Figure 5(a) is the result for $\beta = 2.5\gamma$, it can be found that the number of recovered individuals surpasses the number of suspected individuals roughly at $t = 45$ days. The numbers of exposed individuals and infected individuals reach their peaks at $t = 45$ days. The peaks of the curves E and I are slightly higher and earlier than the model with $\beta = 2.2\gamma$.

Figure 5(b) is the numerical result for the deterministic model with $\beta = 2.0\gamma$. From Fig. 5(b), the number of recovered individuals surpasses the number of suspected individuals roughly after $t = 63$ days, which is later than the model with $\beta = 2.5\gamma$. The numbers of exposed and infected individuals attain their peaks roughly at $t = 60$ days. The peaks of the curves E and I are slightly lower and later than the model with $\beta = 2.5\gamma$.

Figure 5(c) shows the numerical result for the deterministic model with $\beta = 1.5\gamma$ and $t = 150$ days. From this figure, the number of recovered individuals surpasses the number of suspected individuals roughly at $t = 130$ days, which is much later than the model with $\beta = 2.5\gamma$ and $\beta = 2.0\gamma$. The numbers of exposed individuals and infected individuals reach their peaks roughly at $t = 95$ days. The peaks of the curves E and I are much lower and later than the model with $\beta = 2.5\gamma$ and $\beta = 2.0\gamma$.

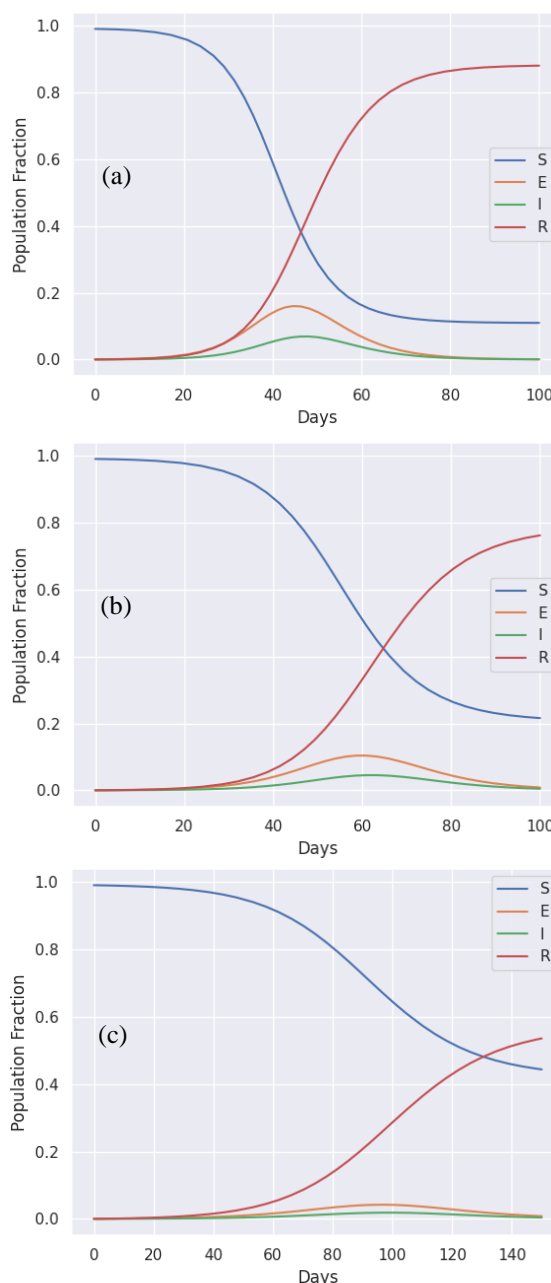


Fig. 5. SEIR model with (a) $\beta = 2.5\gamma$ (b) $\beta = 2.0\gamma$ (c) $\beta = 1.5\gamma$, and $\sigma = 1/5.2$, $\gamma = 1/2.3$, $s(0) = 0.99$, $e(0) = 3(0.02)/100$, $i(0) = 0.02/100$, $r(0) = 0$ and $t = 150$ days.

From Fig. 5, it is observed that when the value of β decreases, the time required for the occurrence of the peaks in the curves E and I become longer, which means that the time span for an epidemic duration becomes longer. Also, the peak values of the curves in categories E and I decrease when β decreases, causing a reduction in the number of individuals who are exposed to and infected with the disease. This implies that when the value of β is small enough, an epidemic outbreak could be expected after a long time, or there may be no epidemic outbreak in the future.

B. Simulation for The SEIR Model Based on A Complete Graph

Based on Fig. 1, since the flow between each category is one-directional, the complete graph seems to be suitable and reasonable for the simulation of a stochastic SEIR model for each category. The movement of each individual from one category to another is a discrete Markov chain, which is a random process. In particular, the discrete Markov chain will enter one of the categories at some point, say category S at time 0, and the process will leave category S and move to category E at time $t > 0$. So, the transition from one category to another is a stochastic process, such that the amount of time it spends in each category before proceeding into the next category follow an exponential distribution with parameter λ . Since the movement from one category to another is exponentially distributed, it is continuous. However, the simulation based on the complete graph is a discrete-time simulation, and thus a geometric distribution is used to replace the exponential distribution.

Also, from the definition of a discrete Markov chain, when the process makes a transition from one category to the next category, there will be a transition probability, denoted as P_{ij} . From Eq. (1), the equations $i'(t) = \sigma e(t) - \gamma i(t)$ and $r'(t) = \gamma i(t)$ imply that there are $\gamma i(t)$ infected individuals that will move from category I to category R . Since γ represents the recovery rate, the probability for an infected individual to become recovered is $q = \gamma\delta$, where δ denotes the time increment. If the generated random number is less than probability q , then that infected individual will move from category I to category R .

The equations from Eq. (1) for categories E and I , which are equations $e'(t) = \beta s(t)i(t) - \sigma e(t)$ and $i'(t) = \sigma e(t) - \gamma i(t)$ also imply that there are $\sigma e(t)$ individuals who transfer from category E to category I . So, the probability for an exposed individual to become infected is $p_2 = \sigma\delta$ since σ is the incubation rate. If the generated random number is less than probability p_2 , then an individual from category E will move into category I .

From Eq. (1), the equations $s'(t) = -\beta s(t)i(t)$ and $e'(t) = \beta s(t)i(t) - \sigma e(t)$ indicate that there are $\beta s(t)i(t)$ individuals in category S who move to category I . Since the exposure rate, λ , equals to $\beta i(t)$, a suspected individual will turn into exposed one with a probability $p_1 = \beta\delta \cdot I[j]$, where $j = 0, 1, \dots, M - 1$ and M denotes the time frame index. So, a suspected individual will turn into exposed one if the generated random number is less than probability p_1 .

The simulation results based on a complete graph for the curves of each category versus time are presented in Fig. 6, in which the total population, N , is 3000, the initial population in category S , $s(0)$ is 0.99, the initial population in category E , $e(0)$ is 0.01, the initial population in category I , $i(0)$ is 0, the initial

population in category R , $r(0)$ is 0, the time domain, T is 60 days, the number of discretization, M , is 4001 and the transmission rate, incubation rate, and recovery rate are set based on [6].

In Fig. 6, the solid line represents the simulation based on a complete graph, while the dashed line represents the deterministic results. After the first few days, the stochastic curve S is above the deterministic curve S , and this remains until $t = 60$ days. The stochastic curve R is lower than the deterministic curve R roughly at $t = 10$ days, and this continues until $t = 60$ days. Although there is a little discrepancy between the stochastic and deterministic results for the categories S and R , they are considered quite close to each other. For the categories E and I , their stochastic and deterministic results are close to each other, and they reach their peaks roughly at $t = 35$ days. Hence, the simulation of the SEIR model based on a complete graph can completely describe and represent the deterministic result.

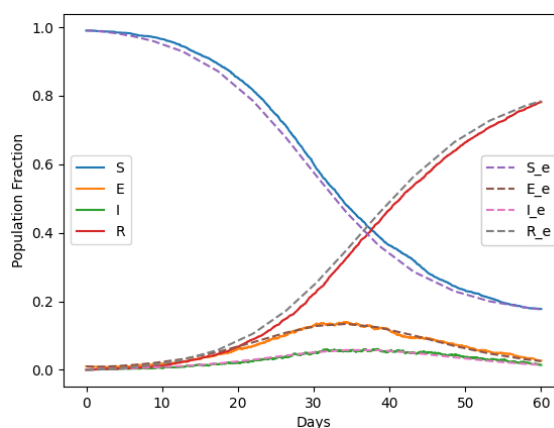


Fig. 6. SEIR model based on a Complete Graph with $N = 3000, \beta = 2.2/2.3, \sigma = 1/5.2, \gamma = 1/2.3, s(0) = 0.99, e(0) = 0.01, i(0) = 0, r(0) = 0, \delta = T / (M - 1), M = 4001$ and $T = 60$ days.

To investigate the effect of the influx of travellers on the results of the SEIR model based on a complete graph, the setting of parameters is the same as in Fig. 6 with additional influxes $a = 0.005$ and $b = 0.001$. However, for each time step t_j of the simulation, the number of individuals in category S will be the sum of the counts of 0 in array C and influx a , while the number of individuals in category E will be the sum of the counts of 1 in array C and influx b . Similarly, the number of individuals in category R will be the counts of -1 in array C subtracted by the sum of influxes a and b .

Figure 7 is the simulation result for the SEIR model based on a complete graph with additional influxes a and b . At the beginning, the stochastic curve S is below the deterministic curve S , but after 20 days, the stochastic curve S surpasses the deterministic curve S and rises above it. At first, the stochastic curve R is above the deterministic curve R , but after the middle of time span, the deterministic curve R surpasses the stochastic curve R , and the deterministic

curve R is again lower than the stochastic curve R , roughly at $t = 52$ days. However, the simulation result for category R is not successful since the stochastic curve R failed to simulate below the value 0 in the beginning stage. For the categories E and I , their stochastic results are below the deterministic result for the whole time domain. Also, the intersection of stochastic curves S and R and the peaks of categories E and I with influxes a and b are slightly earlier than the model without influxes a and b . It is observed that the stochastic result for all the four categories is quite away from the deterministic result and the discrepancy between the stochastic and deterministic results for category S , category E and category R are obvious. Hence, the simulation of SEIR model based on a complete graph with influxes a and b is not successful and it is not as accurate as the deterministic result.

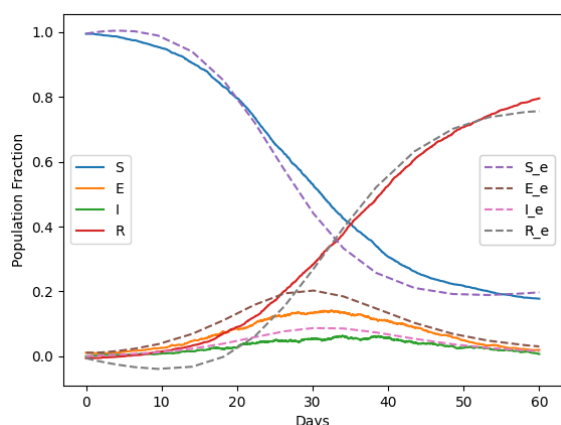


Fig. 7. SEIR model based on a Complete Graph with $N = 3000$, $\beta = 2.2/2.3$, $\sigma = 1/5.2$, $\gamma = 1/2.3$, $s(0) = 0.99$, $e(0) = 0.01$, $i(0) = 0$, $r(0) = 0$, $\delta = T/(M - 1)$, $M = 4001$, $T = 60$ days, $a = 0.005$ and $b = 0.001$.

To see the effect of vaccination rate on the results of SEIR model based on a complete graph, the setting of parameters is identical to that in Fig. 6 except s_0 , e_0 and r_0 are revised into $0.99N(1 - \nu)$, $0.01N(1 - \nu)$ and νN respectively, where ν is 0.30. Figure 8 is the simulation result for the SEIR model based on a complete graph with vaccination rate, $\nu = 0.30$.

From Fig. 8, since the vaccination rate ν is 0.30, it is observed that the initial population in category S is reduced to $0.99(1 - 0.3)$ which equals to 0.693. Similarly, when $t = 0$, the population in category R increases to 0.30. The intersection of stochastic curves S and R is roughly at $t = 50$ days, which are much later than the model without vaccination rate. For the categories E and I , they reach their peaks with values that are much smaller than the simulation without vaccination, roughly at $t = 52$ days. From Fig. 8, it is observed that the stochastic and deterministic curves for the four categories are relatively close to each other. Hence, the simulation of the SEIR model based

on a complete graph with vaccination rate can fully describe the deterministic result.

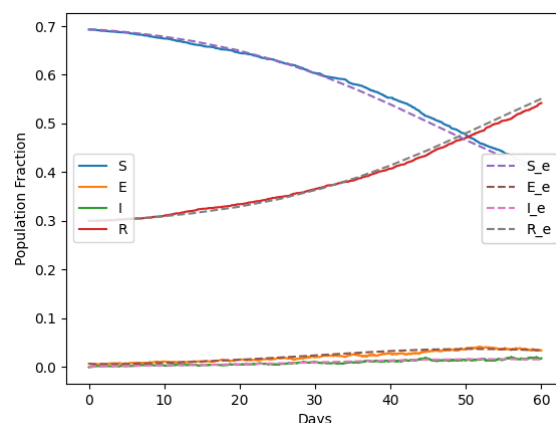


Fig. 8. SEIR model based on a Complete Graph with $N = 3000$, $\beta = 2.2/2.3$, $\sigma = 1/5.2$, $\gamma = 1/2.3$, $\nu = 0.30$, $s(0) = 0.99N(1 - \nu)$, $e(0) = 0.01N(1 - \nu)$, $i(0) = 0$, $r(0) = \nu N$, $\delta = T/(M - 1)$, $M = 4001$ and $T = 60$ days.

C. Simulation for SEIR Model Based on A Steady Graph

In this section, we are going to simulate the stochastic SEIR model using an Erdos-Renyi graph and investigate the outcomes of each category in the SEIR model from a simulation based on a steady Erdos-Renyi graph. An Erdos-Renyi graph is steady if the graph is generated for one time only at the beginning of the simulation, which means that the connection of the nodes in the generated Erdos-Renyi graph will not change for the whole simulation. In the simulation, a $G(n, p)$ model is used to generate the Erdos-Renyi graph, where n is the total number of nodes and p is the edge probability in the graph.

The static probability for the movement of one category to another is the same as the transition probability set in the simulation based on a complete graph, except the probability p_1 is revised into $p_1 = \beta\delta$. In this simulation, contact tracing for the disease with exposed individual and infected individual are being considered, and the probability that an individual becomes exposed and infected becomes dynamic.

The simulation results based on a steady Erdos-Renyi graph for the curves of each category versus time are presented in Fig. 9 with the same parameter setting as Fig. 6 with the addition of the probability used in the Erdos-Renyi graph model $P = \alpha_0/(\alpha_0 + \alpha_1)$, where $\alpha_0 = 1$, $\alpha_1 = d(\alpha_0)/(N - 1 - d)$ and the number of an individual contacts with others, $d = 5.5$. From Fig. 9, it is observed that in the beginning stage, the stochastic result is close to the deterministic result since there is only little randomness that has been taken into account in the model. When the time domain becomes larger, the discrepancy between the deterministic and stochastic results of curves S and R becomes larger.

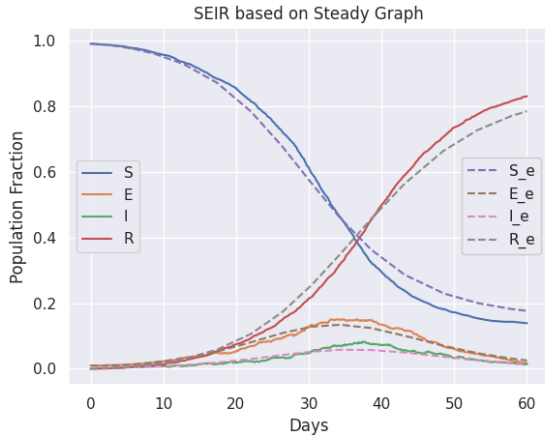


Fig. 9. SEIR model based on a Steady Graph with $N = 3000, \beta = 2.2/2.3, \sigma = 1/5.2, \gamma = 1/2.3, s(0) = 0.99, e(0) = 0.01, i(0) = 0, T = 60$ days and $d = 5.5$.

For category S , the stochastic curve before $t = 38$ days is above the deterministic curve, but after $t = 38$ days, it is lower than the deterministic curve. Before the intersection point of curves S and R , which is roughly at $t = 42$ days, the stochastic curve is below the deterministic curve, but it surpasses the deterministic curve once it passes through the intersection point. The peak of curve E is roughly at $t = 35$ days, while the peak of curve I is rough at $t = 37$ days. Although the simulation of the SEIR model based on a steady graph is not as accurate as the deterministic result, it still has a good performance in describing the deterministic result.

D. Simulation for the SEIR Model Based on a Varying Graph

In this section, the stochastic SEIR model will be simulated based on a varying Erdos-Renyi graph. The simulation process is quite similar to the simulation process based on a steady Erdos-Renyi graph. The main difference between a steady graph and a varying graph is that the connection of the nodes in the varying Erdos-Renyi graph will change randomly for each time step t_j , where $j = 0, 1, \dots, 500$ and the number of discretization, $M = 501$. The setting of parameters and the probability used are the same as in the simulation of the SEIR model based on a steady Erdos-Renyi graph, however after the number of individuals in each category at the current time step is computed, the connection in the graph for the next time step will be reshuffled based on the following:

For each individual i in the total population N and for $k = i + 1, i + 2, \dots, N - 1$,

- i. If node k is not connected to node i , a random number will be generated, and if the generated random number is less than $\alpha_1 \delta$, the connection between node k and node i will be added.
- ii. Conversely, if node k is connected to node i , a random number will be generated, and if the generated random number is less than $\alpha_0 \delta$, the

connection between node k and node i will be removed.

Figure 10 is the simulation result for the SEIR model based on a varying Erdos-Renyi graph. It is observed from Fig. 10 that in the beginning stage, the stochastic result for all the categories seems to be close enough to the deterministic result. However, as time goes by, the discrepancy between the deterministic and stochastic results is getting larger because the randomness involved in the model becomes larger. The stochastic curve S becomes lower than the deterministic curve S roughly after 10 days, and the discrepancy between the deterministic and stochastic results in the category S becomes larger. After 20 days, the stochastic curve R surpasses the deterministic curve R and when the time duration becomes longer, the discrepancy between the deterministic and stochastic curve R is getting larger. Also, the intersection between the curves S and R for the stochastic result is earlier than the deterministic result. Although there are few discrepancies between the peaks of the stochastic and deterministic curves E and I , they can be considered close enough to the deterministic result compared to curves S and R .

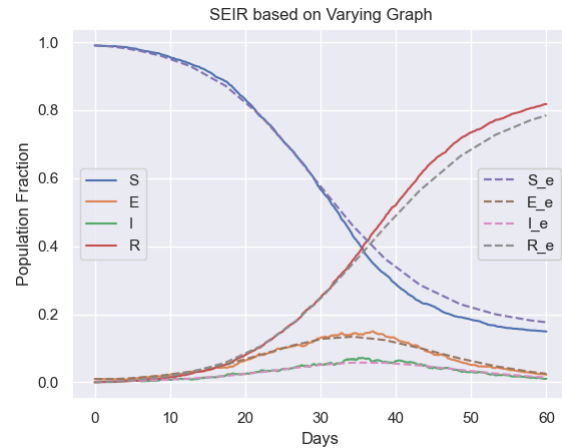


Fig. 10. SEIR model based on a Varying Graph with $N = 3000, \beta = 2.2/2.3, \sigma = 1/5.2, \gamma = 1/2.3, s(0) = 0.99, e(0) = 0.01, i(0) = 0, T = 60$ days and $d = 5.5$.

IV. CONCLUSION

In this paper, the SEIR model, which is a mathematical model that commonly used to describe the spread of an epidemic disease, is used in the present study to evaluate the number of individuals who are suspected, exposed, infected, and recovered for/from a disease based on the transmission rate, incubation rate, and recovery rate. The strength of SEIR model is that it is more realistic than the SIR model as it can help us understand the impact of isolating exposed individuals on the dynamics of disease spread. The results of the deterministic SEIR model and stochastic SEIR model based on complete graphs, steady Erdos-Renyi graphs and varying Erdos-Renyi graphs are analysed and compared. The changes in the results for both the deterministic and stochastic

SEIR models when other factors such as vaccination rate and inflow or outflow rate due to travelling are explored. Among the stochastic models, the simulation based on the complete graph is more consistent with the deterministic result.

When the value of the transmission rate decreases, the peaks of the number of exposed and infected individuals are reduced and moved farther out in time. However, while the value of the transmission rate decreases to a value that is small enough, making the basic reproductive number, R_0 , to be less than one, no epidemic outbreak is expected. Hence, the SEIR model indicates that control measures such as social distancing, limiting non-essential travel, wearing masks in public areas and vaccination campaigns are useful to reduce the number of exposures and infections of spreading disease and could effectively avoid the occurrence of pandemic outbreaks.

Due to the limitation of time and scope, only a simpler SEIR model with influxes a and b are considered in this study to simulate the population distribution and flow among each category via Complete Graph and Erdos-Renyi graph theories. However, for many respiratory infections, immunity after recovery is generally temporary and recovered individuals will probably lose immunity and thus return to suspected state (S) after a protected period. In addition, death toll due to infection will cause a loss of individuals from the I group, meanwhile, all groups will also experience background death from other causes at a certain rate. Therefore, the loss of immunity, rate of births and deaths are also important factors when it comes to a SEIR epidemic outbreak model as they can contribute to susceptible recruitment into the state S and create an 'open epidemic' status. Possible future work for the current study might reside on the extensions of the current SEIR model by introducing several extra components such as rate of immunity loss, rate of death due to infection and other cause, rate of vaccination and the age of category individual. A more complicated set of ordinary differential equations might occur, and the simulation process might need to be refined, moreover, other available random processes might need to be explored in order to deal with the complicated SEIR nature.

ACKNOWLEDGEMENT

This research was partially supported by the Xiamen University Malaysia in Malaysia through Xiamen University Malaysia Research Fund (XMUMRF) with Grant No: XMUMRF/2018-C2/IMAT/0005. The authors are grateful for this support.

REFERENCES

- [1] M. R. K. Ariffin, K. Gopal, I. Krishnarajah, I. S. C. Ilias, M. B. Adam, J. Arasan, N. H. A. Rahman, N. S. M. Dom and N. M. Sham, "Mathematical Epidemiologic and Simulation

- Modelling of First Wave COVID-19 in Malaysia," *Sci. Rep.*, vol. 11, no. 20739, 2021.
- [2] J. M. Carcione, J. E. Santos, C. Bagaini and J. Ba, "A Simulation of A COVID-19 Epidemic Based on A Deterministic SEIR Model," *Frontiers in Public Health*, vol. 8, no. 230, 2020.
- [3] D. Dansana., R. Kumar, A. Parida, R. Sharma, J. D. Adhikari, H. V. Le, B. T. Pham, K. K. Singh and B. Pradhan, "Using Susceptible-Exposed-Infectious-Recovered Model to Forecast Coronavirus Outbreak," *Comput., Mat. & Cont.*, vol. 67, no. 2, pp. 1595–1612, 2021.
- [4] V. Piccirillo, "Nonlinear Control of Infection Spread Based on A Deterministic SEIR Model," *Chaos, Solitons & Fractals*, vol. 149, 111051, 2021.
- [5] R. Ghostine, M. Gharamti, S. Hassrouny and I. Hoteit, "An Extended SEIR Model with Vaccination for Forecasting the COVID-19 Pandemic in Saudi Arabia Using an Ensemble Kalman Filter," *Mathematics*, vol. 9, no. 636, 2021.
- [6] J. Gopalakrishnan, "The SEIR Model of Infectious Diseases," https://web.pdx.edu/~gjay/teaching/mth271_2020/html/09_SEIR_model.html [accessed 25 April 2022].